

Prospects for Detection of Intracluster Gas Bulk Velocities Through the Sunyaev-Zel'dovich Effect

Renato A. Dupke & Joel N. Bregman

Department of Astronomy, University of Michigan, Ann Arbor, MI 48109-1090

ABSTRACT

Intracluster gas velocity gradients have been recently detected by the authors in the Centaurus cluster (Abell 3526) using the Doppler shift of X-ray spectral lines with *ASCA* Solid-state Imaging Spectrometers. The velocity gradient was found to be maximum along a line roughly perpendicular to the direction of the incoming subgroup Cen 45 and has a correspondent velocity difference of $\sim 3.4 \pm 1.1 \times 10^3 \text{ km s}^{-1}$ within a $\sim 10'$ -diameter region centered on the cD galaxy NGC 4696. Such bulk velocities should Comptonize the Cosmic Microwave Background Radiation producing variations of intensity and temperature that can be detectable in the near future with bolometers such as BOLOCAM. In this paper we realistically estimate the expected CMBR Comptonization for the central region of Abell 3526, using *ASCA* and *ROSAT* data to constrain the S-Z parameter expectations.

Subject headings: galaxies: clusters: individual (Abell 3526) — intergalactic medium — cooling flows — X-rays: galaxies: clusters — cosmology: cosmic microwave background

1. Introduction

Clusters of galaxies are believed to form from the infall/merging of smaller scale systems. Memory of the formation process may be probed through the X-ray analysis of the intracluster medium (ICM), where most of the cluster's visible mass resides. This is due to the fact that the merging of sub-units is predicted to create gas substructures such as temperature and density inhomogeneities, destruction of cooling flows & metal abundance gradients and generation of gas bulk velocities. The comparison of observed structures to numerical hydrodynamical+N body simulations can then provide clues as to the cluster's evolutionary stage (e.g. Evrard 1990; Katz & White 1993; Navarro, Frenk & White 1995;

Evrard, Metzler, & Navarro 1996; Roettiger, Burns & Loken 1993,1996; Schindler & Muller 1993; Pearce, Thomas & Couchman 1994; Gomez et al. 2001 and references therein).

Until very recently the physical characteristics of the ICM had been derived almost exclusively by the analysis of distributions of electron temperature (T_e) and surface brightness (S_X) (or gas density), even though in the last few years various numerical simulations of off-center cluster mergers have been published predicting the presence of long-lasting residual intracluster gas velocities approaching a few thousand km s^{-1} (e.g. Roettiger, Loken & Burns 1997, Ricker 1998; Roettiger, Stone, & Mushotzky 1998; Takizawa & Mineshige 1998; Burns et al. 1999; Takizawa 1999, 2000; Roettiger & Flores 2000). Furthermore, since we are always looking at 2-D projections, velocity maps may be a crucial addition, necessary to break the degeneracies associated with analyses based solely on T_e & S_X distributions.

Recently, Dupke & Bregman (2001a,b) detected ICM bulk motions in two galaxy clusters using *ASCA* data: Perseus (Abell 426) and Centaurus (Abell 3526). The intracluster gas velocity distributions detected in these two clusters are roughly consistent with systematic gas bulk rotation with correspondent circular velocities $> 1000 \text{ km s}^{-1}$, implying that a significant fraction of the intracluster gas energy can be kinetic. Since X-ray measurements are haunted by the need of precise knowledge of instrumental gain ¹ these detections are significant only at the (2-4) σ level. Realistically, the significance of these measurements are not expected to improve substantially within the next several years even with *Chandra* and *XMM-Newton*, since the spectral resolution of the imaging spectrometers on-board these satellites, ACIS and EPIC², is only slightly better than that of the SISs on-board *ASCA*. Furthermore, it will take a few years before detailed gain variations across those detectors are known well enough for reliable ICM velocity measurements. To compensate for the lack of knowledge of the gain variations in X-ray spectrometers it is necessary to take several consecutive off-center long-exposure observations of a cluster, so that sky regions with discrepant radial velocities can be observed at the same CCD position. However, this kind of measurement is very time consuming if one does not have prior knowledge of the best orientations for velocity measurements.

Alternatively, ICM velocity measurements can be, in principle, corroborated/detected by the use of the kinetic S-Z effect (Sunyaev & Zel'dovich 1970, 1972, 1980). Intracluster gas bulk velocities as high as those detected in A3526 should generate significantly different

¹conversion between pulse height and incoming photon energy

²We are not considering the gratings since they are less suited for this kind of spatially-resolved spectroscopy

levels of Comptonization of the cosmic microwave background radiation (CMBR) towards different direction of the cluster (red-shifted and blue-shifted sides). This effect could be detected with current (or in development) instruments, such as the *BOLOCAM*³, or, with smaller spatial resolution, *ACBAR*⁴ and the High Frequency Instrument on-board *PLANCK*⁵.

In this paper we realistically predict differential variation of the CMBR temperature as it passes through the intracluster gas of the central regions of the Centaurus cluster, $(\frac{\Delta T}{T})_{CMBR} \sim 10^{-4}$. We propose that this effect can be observed soon in cool clusters such as Centaurus at frequencies that minimize the thermal component (214 GHz). We suggest that differential S-Z measurements of clusters, coupled with X-ray spatially resolved spectroscopy can provide crucial information not just to cosmology but also to the study of intracluster gas dynamics.

2. The Mechanism

The CMBR intensity and temperature variations with respect to the background towards the direction of a rotating cluster has two components; a thermal and a kinetic component. The latter can be associated with some global peculiar velocity and also with internal bulk motions, which is the one that we are interested in this work. If the resulting radial velocity of the kinetic S-Z component at some projected radius “b” is denoted by V_r the thermal and kinetic variation of intensity (I) and temperature (T) of the CMB in the non-relativistic approximation can be given by (for reviews see, e.g., Rephaeli 1995; Birkinshaw 1999):

$$\Delta I_\nu \approx 2 \frac{(kT)^3}{(hc)^2} \frac{x^4 e^x}{(e^x - 1)^2} (K(T_e, \nu) - \beta_r(b)) \tau(b) \quad (1)$$

$$\left(\frac{\Delta I}{I}\right)_\nu \approx \frac{x e^x}{e^x - 1} (K(T_e, \nu) - \beta_r(b)) \tau(b) \quad (2)$$

$$\left(\frac{\Delta T}{T}\right)_\nu \approx (K(T_e, \nu) - \beta_r(b)) \tau(b) \quad (3)$$

³www.astro.caltech.edu/~igg/bolocam/bolocam.html

⁴astrophysics.phys.cmu.edu/research/viper/

⁵astro.estec.esa.nl/Planck/

where

$$K(T_e, \nu) = \frac{kT_e}{m_e c^2} \left(x \frac{e^x + 1}{e^x - 1} - 4 \right) \quad (4)$$

$$\beta_r(b) = \frac{V_r(b)}{c} \text{ and } x = \frac{h\nu}{kT} \quad (5)$$

where T_e & T are respectively the ICM and CMB temperatures, and the other parameters have their usual meanings. If the gas number density $n(r)$ follows a king-like profile $n(r) = n_0(1 + (\frac{r}{r_c})^2)^{-\frac{3}{2}\beta}$, where r_c and n_0 are respectively the core radius and the central density, the optical depth is given as a function of the projected radius “b” by

$$\tau(b) = \sigma_T n_0 r_c B\left(\frac{1}{2}, \frac{3}{2}\beta - \frac{1}{2}\right) \left(1 + \left(\frac{b}{r_c}\right)^2\right)^{-\frac{3}{2}\beta + \frac{1}{2}} \quad (6)$$

where $B(p, q) = \int_0^\infty x^{p-1} (1+x)^{p+q} dx$ is the Beta function of p,q.

3. The Case for Abell 3526

Centaurus (Abell 3526) is a BM type I, nearby ($z \sim 0.0104$), X-ray bright cooling flow (accretion rate $< 30\text{-}50 M_\odot \text{yr}^{-1}$), cold ($kT_e \sim 3\text{-}3.5 \text{ keV}$) cluster. Its X-ray emission is relatively smooth except for the central $1'$ where *Chandra* found X-ray substructures (Sanders & Fabian 2001), and is peaked on the cD galaxy NGC 4696. The existence of galaxy velocity bi-modality in Centaurus had been shown by Lucey, Currie & Dickens (1986a,b) and was more recently confirmed by Stein et al. (1997). Two galaxy groups are clearly separated: the main group (Cen 30), which is centered on the cD galaxy (NGC 4696) shows an average radial velocity of $3397 \pm 139 \text{ km s}^{-1}$ and a velocity dispersion of $933 \pm 118 \text{ km s}^{-1}$. The second group (Cen 45) is associated with the galaxy NGC 4709 at $\gtrsim 15'$ from NGC 4696. It has an average radial velocity of $4746 \pm 43 \text{ km s}^{-1}$ and a velocity dispersion of $131 \pm 43 \text{ km s}^{-1}$. One arcmin at Centaurus distance corresponds to $\sim 19 h_{50}^{-1} \text{ kpc}$. The general interpretation for this bi-modality is that Cen 45 is being accreted by the Centaurus cluster. This explanation has been further strengthened by: 1) the discovery of higher gas temperatures ($\gtrsim 5 \text{ keV}$) associated with Cen 45 by Churazov et al. (1999) and 2) a marginally significant intracluster gas velocity difference of $\sim 1800 \text{ km s}^{-1}$ between Cen 45 and Cen 30 detected by Dupke & Bregman (2001b), hereafter DB01.

More interestingly, DB01 found a small-scale (within the central $10'$) significant ($>99.8\%$ confidence) intracluster gas velocity gradient more or less symmetric with respect

to the cluster’s center, consistent with bulk gas rotation with a correspondent circular velocity of $1.59 \pm 0.32 \times 10^3 \text{ km s}^{-1}$. The nature of this velocity gradient is likely to be related to some previous merger on the main body of the Centaurus cluster (Cen 30). The maximum velocity difference is found roughly along an axis at a position angle of $\sim 40^\circ$ (Figure 1). Therefore, velocity measurements by means of the kinetic S-Z effect on CMBR temperature and intensity variations could be optimized along that axis (e.g. by choosing symmetric subregions for source/background along that position angle, such as the extremes of the box in Figure 1).

In Figure 2 we show the absolute and relative variations of intensity and CMBR temperature towards the directions of maximum (dotted) and minimum (dashed) velocities *as observed* by ASCA, i.e., $5'$ away from the cluster’s core (regions P3 & P7 in Figure 1), as a function of wavelength. Both kinetic and thermal effects are added. The gas density profile used was obtained taking into account that we are looking at spatial regions with the same scale as (or smaller than) the cluster’s core radius. Therefore, it is more appropriate to choose surface brightness profile fittings that realistically take into account the central cluster region, where the surface brightness is enhanced and single β models diverge significantly from the observed profiles. We believe that the double β fitting profiles used in the extensive *ROSAT* analysis of Mohr, Mathiesen & Evrard (1999) (hereafter MME99) are the most reliable for that purpose and we use them in our calculations⁶

MME99 surface brightness fitting function $S_X(b) = \sum_{i=1}^2 S_{X0_i} (1 + (\frac{b}{r_{c_i}})^2)^{-3\beta + \frac{1}{2}}$, assumed a constant β but different core radii and normalizations for the dominant components near the center and away from the central regions. To deproject that surface brightness fitting and obtain a “physical” density profile MME99 expressed the total gas density as being proportional to the primary density component multiplied by a “fudge” function ($f(r)$) that compensated for the distortions caused by the central component. MME99 constrained $f(r)$ using the observed surface brightness for each radial bin. Following their methodology we use for our $\tau(b)$ the following integral

$$\tau(b) = 2\sigma_T \frac{n_{e0}}{f(0)} \int_b^\infty (1 + (\frac{r}{r_{c1}})^2)^{-\frac{3}{2}\beta} \frac{f(r)rdr}{\sqrt{r^2 - b^2}} \quad (7)$$

instead of Equation 6. In Equation 7 n_{e0} and $f(0)$ are the number density and the “fudge” function ($f(r)$) at the cluster’s center (MME99). We use for the functional form of $f(r)$ an inverse polynomial given as $f(r > 1') \cong \text{const0} + \frac{\text{const1}}{b} + \frac{\text{const2}}{b^2}$, where the

⁶The choice of MME99 is also a conservative one, since other surface-brightness-derived density profiles available in the literature, e.g. Jones & Forman 1999, typically produce higher values for the optical depth within the spatial regions considered, thus enhancing the magnitude of $\frac{\Delta T}{T}$.

best fit values within $b < 190 h_{50}^{-1}$ kpc are $const0 = 0.817$, $const1 = 1.05 \times 10^{23} cm$ & $const2 = 2.7 \times 10^{46} cm^2$.

The surface brightness parameters used to derive the optical depth (Equation 7) are $T_e(r=5') = 3.4$ keV, $V_{circ}(r=5')=1600$ km s⁻¹ (DB01), $\beta=0.57$, $n_{e0}=0.068$ cm⁻³, $r_{c1}=7.3'$ (MME99). In all three plots the solid thick line shows the difference between the redshifted and blueshifted curves. It can be seen that the CMBR intensity variation difference (Figure 2, Top) is maximized at 214 GHz ($\lambda=0.14$ cm). This is the optimal frequency to observe the relative kinetic S-Z effect and consequently to determine a velocity map. At that frequency the difference between the relative variations of intensity and temperature are $\Delta(\frac{\Delta I}{I}) \sim 5 \times 10^{-4}$ and $\Delta(\frac{\Delta T}{T}) \sim 10^{-4}$ (Figure 2 middle and bottom plots).

The magnitude of the parameters derived above are, naturally, a function of the projected radial distance from the cluster’s center. In order to determine the radial profile of the expected $\frac{\Delta T}{T}$ at 214 GHz we make two assumptions; Firstly, we assume that in the region from 0’ to 5’ the cooling flow can be approximated by a linear function varying from 3.4 keV to 1 keV at the center. The flattening of the temperature profile at the cluster’s center has been observed for some clusters with *Chandra* and *XMM*, and may be a common feature of cooling flows (Fabian 2001). In the case of Centaurus there is evidence that the minimum temperature derived from spectral fittings using cooling flow models is > 0.4 -1.0 keV (Sanders and Fabian 2001). The central arcmin in Centaurus has an impressive amount of substructures (plumes) and this makes our estimation of the central densities more uncertain. Therefore, we exclude that region from our analysis (Figure 3). Secondly, we assume the gas motion can be approximated by a solid body rotation. This functional form for the gas velocity cannot be supported for larger radii since the gas becomes gravitationally unbound but it is a good observed first order approximation for the inner regions (Dupke & Bregman 2002). Actually, this assumption is supposed to break at ~ 5 -6’, when the combined bulk kinetic and thermal energies become greater than the gravitational and the gas becomes unbound (e.g. see Allen & Fabian 1994). Assuming that the velocity “freezes” at 1600 km s⁻¹, we also show in Figure 3 the predicted behavior of $\frac{\Delta T}{T}$ at regions radially greater than that encompassed by ASCA velocity analysis, for illustration purposes.

The kinetic Comptonization of the spectrum that reaches us from a rotating cluster is roughly antisymmetric with respect to the center of the cluster from ~ 160 -270 GHz. This suggests that larger variations of intensity and temperature of the CMBR can be observationally enhanced by comparing the measurements (in the same channel) “within” the cluster, rather than to a background region away from the cluster. The results are maximized at 214 GHz and we show the distribution of CMB temperature variations

($\frac{\Delta T}{T}(b)$) at that frequency in Figure 3. The horizontal errors in Figure 3 show the FWHM of BOLOCAM. The solid lines represent the estimated $1-\sigma$ errors of measurement associated to the X-ray-derived parameters, and are dominated by X-ray velocity measurement errors. S-Z measurements of radial velocities can be performed within these $1-\sigma$ limits with a relatively short exposure time (see below).

Variations of intensity or temperature of that magnitude can be relatively easily observed currently, or in the very near future, with the new generation of bolometers. A total variation of CMB temperature of ~ 0.3 mK between the “knees” in Figure 3 is equivalent to a flux density of $\Delta I_{lim} \sim 1.2$ mJy (FWHM)⁻², This could be done with high significance in a relatively short amount of time with, for example, *BOLOCAM*, given that for that instrument the FWHM is $43''$ and the *expected*⁷ noise equivalent flux density (NEFD) is 35 mJy Hz^{-1/2} at the 1.4mm band⁸(Glenn et al. 1998).

4. Summary

Direct indications of the presence of large bulk motions in clusters of galaxies have been recently obtained through X-ray spatially resolved spectroscopy. However, these observations are limited by detector’s gain fluctuations and this will continue to be the case for the next several years. An alternative way of measuring intracluster gas bulk velocities is through the use of the kinetic S-Z effect. The use of bolometers has improved significantly the precision of radio observations of the S-Z effect, especially within the optimal frequency range for such measurements, i.e., ~ 214 GHz ($\lambda = 0.14$ cm), so that, it will be possible in the near future to perform such velocity measurements in instruments such as *BOLOCAM* (Bock et al 1998) with relatively short exposure times. The combination of X-ray and radio measurements can provide us with independent/complementary information crucial to build ICM velocity maps and to determine the degree of evolution and the history of galaxy clusters.

So far, the best candidate for testing the proposed multi-wavelength measurements of velocity gradients is the Centaurus cluster. The symmetry of the gas velocity distribution and the low temperatures measured for this cluster should facilitate the separation of the rotational kinetic component from both thermal and peculiar velocity ones. By combining

⁷Samantha Edgington and the Bolocam Team, Personal Communication

⁸The nominal observation time necessary to detect a limiting flux density I_{lim} is $t_{obs} \sim (\frac{NEFD}{\Delta I_{lim}})^2$ sec plus overhead

the analyses of intracluster gas velocity & temperature distributions with other relevant X-ray cluster characteristics we predict that the variations of CMBR temperature between two regions symmetrically located $5'$ from the clusters center along the line of maximal velocity gradient at $\lambda = 0.14$ cm is ~ 0.3 mK.

The magnitude of the S-Z parameters observationally derived in this work, if typical, could significantly enhance possible halo-induced gas rotation contribution to the CMBR angular power spectrum (Cooray & Chen 2002). However, the limiting nature of the search for velocity gradients using current X-ray spectrometers tends to be biased towards clusters with high bulk velocities, so that the current data does not allow us yet to calculate precise velocity distributions and, consequently, to determine the deviations from the assumptions used in statistical analysis of the temperature anisotropies such as those performed by Cooray & Chen (2002). Furthermore, if both “rotational” and “transient” bulk velocities are as common in the central regions of clusters as suggested by a more extended ASCA analysis (Dupke & Bregman 2002), measurements of cluster peculiar velocities using the S-Z effect should be treated with extreme caution, given the potential confusion with an internal gas bulk motion component.

Multiple off-center long exposure velocity measurements of intracluster gas with the *Chandra* and *XMM-Newton* satellites coupled with radio observations of the differential kinetic S-Z effect will be crucial to determine precise intracluster velocities in the central and intermediate regions of galaxy clusters, improving significantly the determination of their evolutionary stage, and constraining biases related to the presence of coherent velocity fields in blind S-Z surveys.

We are very grateful to Frits Paerels and Gary Bernstein for the helpful discussions and constructive suggestions. We would like to thank Joe Mohr for kindly providing the tabulated distribution of the “fudge” function that was used in this paper. We also thank Samantha Edgington and the Caltech BOLOCAM team for helpful suggestions. We thank Hugh Aller & Tim Paglione for helpful discussions. We acknowledge support from NASA Grant NAG 5-3247. This research made use of the HEASARC ASCA database and NED.

REFERENCES

- Allen, S. W. & Fabian, A. C. 1994, MNRAS, 269, 409
Birkinshaw, M. 1999, Phys. Rep., 310, 97
Bock, J. J., Chattopadhyay, G., Edgington, S. F., Lange, A. E., Zmuidzinas, J., Mauskopf,

- P. D. Rownd, B., Yuen, L., and Ade, P. A. R. 1998, Proc. SPIE Vol. 3357, p. 326-334
- Burns, J. O., Loken, C., Roettiger, K., Rizza, E., Bryan, G., Norman, M. L., Gomez, P. and Owen, F. N. 1999, "Life Cycles of Radio Galaxies", ed. J. Biretta et al., New Astronomy Reviews, astro-ph/9908361
- Churazov, E., Gilfanov, M., Forman, W., & Jones, C. 1999, ApJ, 520, 105
- Cooray, A. & Chen, X. 2002, ApJ in press, astro-ph/0107544
- Dupke, R. A., & Bregman, J. N. 2001a, ApJ, 547, 705.
- Dupke, R. A., & Bregman, J. N. 2001b, ApJ, 562, 266 (DB01).
- Dupke, R. A., & Bregman, J. N. 2002, in preparation.
- Evrard, A. E. 1990, ApJ, 363, 349;
- Evrard, A. E., Metzler, C. A., & Navarro, J. F. 1996, ApJ, 469, 494;
- Fabian, A. 2001, in in *Lighthouses of the Universe* eds. M. Gilfanov, R. Sunyaev et al., Springer-Verlag, astro-ph/0201386
- Glenn, J., et al. 1998, Proc. SPIE Vol. 3357, p. 326-334
- Gomez, P. L., Loken, C., Roettiger, K., & Burns, J. O. 2001, ApJ, in press (astro-ph/0009465)
- Jones, C., & Forman, W. 1999, ApJ, 511, 65
- Katz, N., & White, S. D. M. 1993, ApJ, 412, 455;
- Lucey, J. R., Currie, M. J., & Dickens, R. J. 1986a, MNRAS, 221, 453
- Lucey, J. R., Currie, M. J., & Dickens, R. J. 1986b, MNRAS, 222, 427
- Mohr, J. J., Mathiesen, B. & Evrard, A. 1999, ApJ, 517, 627 (MME99)
- Navarro, J. F., Frenk, C. S., & White, S. D. M. 1995 MNRAS, 275, 720
- Pearce, F. R., Thomas, P. A., & Couchman, H. M. P. 1994, MNRAS, 268,953;
- Rephaeli, Y. 1995, ARA&A, 33, 541
- Ricker, P. M. 1998, ApJ, 496, 670
- Roettiger, K., Burns, J. O., & Loken, C. 1993, ApJ, 407, 53;
- Roettiger, K., Burns, J. O., & Loken, C. 1996, ApJ, 473, 651
- Roettiger, K., Loken, C., & Burns, J. O. 1997, ApJS, 109, 307
- Roettiger, K., Stone, J. M. & Mushotzky, R. 1998, ApJ, 1493, 62

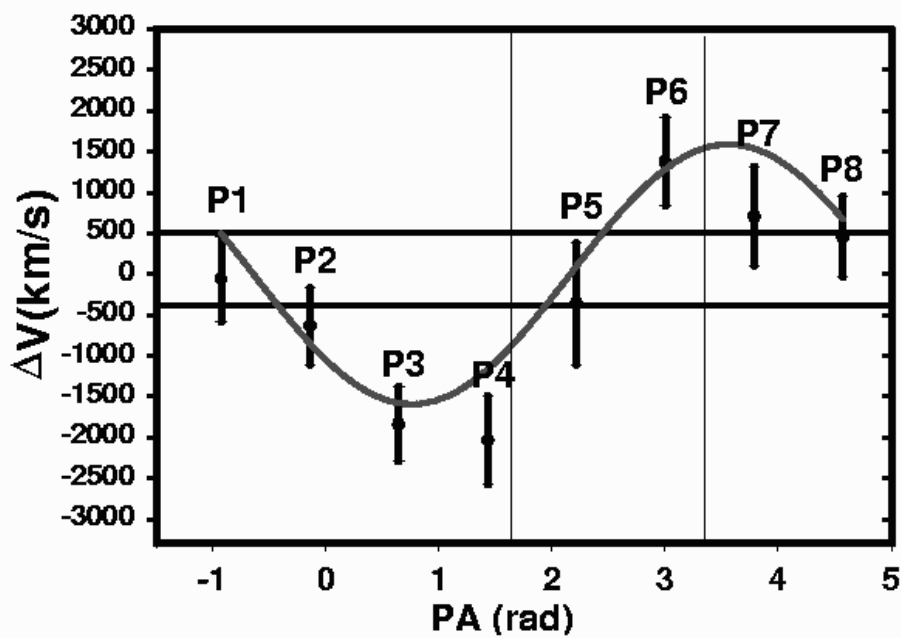
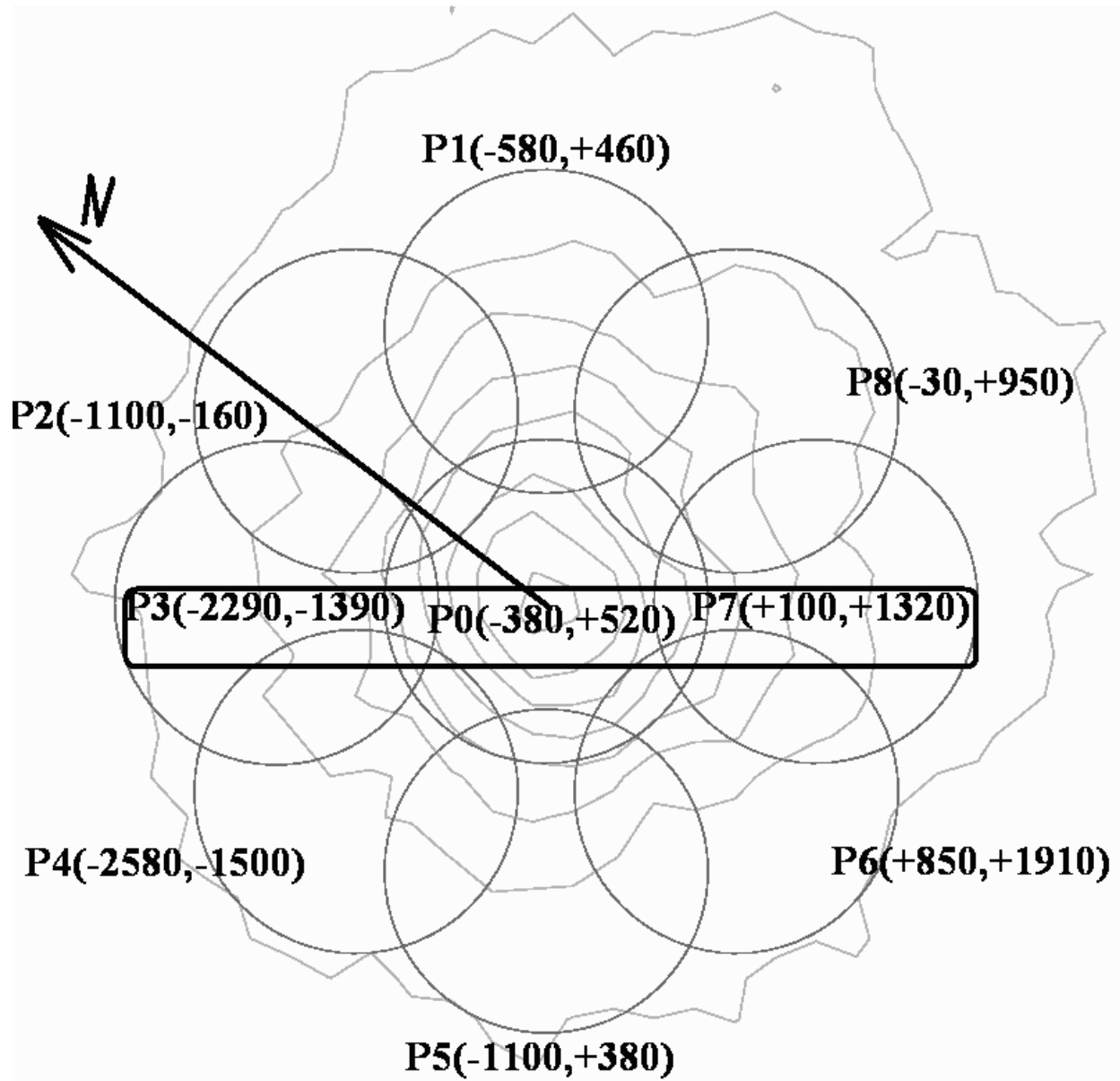
- Roettiger, K. & Flores, R. 2000, ApJ, 538, 92
- Sanders, J. S. & Fabian, A. C. 2001, MNRASsubmitted (astro-ph/0109336)
- Schindler, S., & Muller, E. 1993, A&A, 272, 137 ;
- Stein, P., Jerjen, H., & Federspiel, M. 1997, A&A, 327, 952
- Sunyaev, R. A., & Zel'dovich, Ya. B. 1970, Astrophys. Space Sci., 7, 3
- Sunyaev, R. A., & Zel'dovich, Ya. B. 1972, Comments Astrophys. Space Phys., 4, 173
- Sunyaev, R. A., & Zeldovich, Ya. B. 1980, MNRAS, 190, 413
- Takizawa, M., & Mineshige, S. 1998, ApJ, 499, 82;
- Takizawa, M. 1999, ApJ, 520, 514
- Takizawa, M. 2000, ApJ, 532, 183

Figure Captions

Fig. 1.— Radial Velocity Distribution in Centaurus. (TOP) ASCA GIS X-ray surface brightness overlaid by the regions analyzed by Dupke & Bregman (2001b). The values in parenthesis indicate the 1σ confidence limits for one interesting parameter (velocities). The box shows the region of maximum velocity gradient according to a solid body rotation fit. "N" denotes the Northern direction. (Bottom) with an associated circular velocity of 1600 km s^{-1} . The vertical lines indicate the direction of the incoming subgroup Cen45. The two horizontal lines show the 1σ confidence limits for the velocity measured in the central region P0.

Fig. 2.— Intensity and temperature variations as a function of wavelength for two regions symmetrically located $5'$ from Centaurus' center along the direction perpendicular to the apparent rotation axis. The long-dashed & dotted lines in all plots represent the curves for negative and positive values of radial velocity (V_r), respectively. The dashed-dotted line in the TOP plot shows the case for the thermal contribution alone ($V_r=0$). We also show the intensity variations for the kinetic component alone ($T_e=0$) in the TOP plot only, for illustration, and long-dashed & dotted lines have the same meaning as described before. The solid line in all plots shows the magnitude of the difference between the negative and positive V_r (differential variations). For intensity variations (Top plot) this difference achieves a maximum at $\lambda=0.14 \text{ cm}$ ($\nu=214 \text{ GHz}$).

Fig. 3.— $\frac{\Delta T}{T}$ at $\lambda = 0.14 \text{ cm}$ radial dependence along the direction of maximum velocity gradient. The solid lines indicate the $1-\sigma$ errors correspondent to the ICM velocities measured by ASCA. The horizontal errors indicate the FWHM of BOLOCAM for illustration purposes. The velocity profile is assumed to have a solid body form up to $\sim 5'$ and then to be constant at 1600 km s^{-1} . The dotted line shows the expected temperature variation for the thermal component alone.



Centaurus NR S-Z
R = 5'; T = 3.4 keV; V_{circ} = 1600 km/s

